Estuaries and Coasts (2016) 39:916–934
DOI 10.1007/s12237-015-0057-x

Evolution of Mid-Atlantic Coastal and Back-Barrier Estuary Environments in Response to a Hurricane: Implications for Barrier-Estuary Connectivity

Jennifer L. Miselis[1] · **Brian D. Andrews**[2] · **Robert S. Nicholson**[3] · **Zafer Defne**[2] · **Neil K. Ganju**[2] · **Anthony Navoy**[3]

Received: 24 August 2015 / Revised: 4 November 2015 / Accepted: 22 November 2015 / Published online: 29 December 2015

Abstract Assessments of coupled barrier island-estuary storm response are rare. Hurricane Sandy made landfall during an investigation in Barnegat Bay-Little Egg Harbor estuary that included water quality monitoring, geomorphologic characterization, and numerical modeling; this provided an opportunity to characterize the storm response of the barrier island-estuary system. Barrier island morphologic response was characterized by significant changes in shoreline position, dune elevation, and beach volume; morphologic changes within the estuary were less dramatic with a net gain of only 200,000 m^3 of sediment. When observed, estuarine deposition was adjacent to the back-barrier shoreline or collocated with maximum estuary depths. Estuarine sedimentologic changes correlated well with bed shear stresses derived from numerically simulated storm conditions, suggesting that change is linked to winnowing from elevated storm-related wave-current interactions rather than deposition. Rapid storm-related changes in estuarine water level, turbidity, and salinity were coincident with minima in island and estuarine widths, which may have influenced the location of two barrier island breaches. Barrier-estuary connectivity, or the transport of sediment from barrier island to estuary, was influenced by barrier island land use and width. Coupled assessments like this one provide critical information about storm-related coastal and estuarine sediment transport that may not be evident from investigations that consider only one component of the coastal system.

Keywords Barnegat Bay · Hurricane Sandy · Coastal change · Water quality · Geomorphology · Sediments · Numerical modeling

Communicated by David Reide Corbett

✉ Jennifer L. Miselis
jmiselis@usgs.gov

[1] St. Petersburg Coastal and Marine Science Center, US Geological Survey, 600 4th St. S, St. Petersburg, FL 33701, USA

[2] Woods Hole Coastal and Marine Science Center, US Geological Survey, 384 Woods Hole Rd., Woods Hole, MA 02543, USA

[3] New Jersey Water Science Center, US Geological Survey, 3450 Princeton Pike, Suite 110, Lawrenceville, NJ 08648, USA

Introduction

Given the likelihood of increases in the rates of sea level rise (Church and White 2011; Gregory et al. 2013; Vermeer and Rahmstorf 2009) and the possibility of future increases in the intensity of tropical cyclones and associated rainfall in some coastal areas (Knutson et al. 2010), identifying the controls on and magnitude of storm-induced sediment transport is critical for understanding future coastal evolution. Barrier islands, globally distributed but more common along passive margins (McBride et al. 2013; Stutz and Pilkey 2001), are especially vulnerable to sea level rise and storms due to their relatively low elevations and their position between the ocean and the mainland. It is widely accepted that barrier island rollover, the process in which sediment is transported from the littoral zone and deposited landward, is the primary mechanism by which barrier islands keep up with sea level rise (Dolan and Godfrey 1973; Donnelly et al. 2006; McBride et al. 2013). Recent morphologic behavior modeling demonstrates the importance of estuary morphology and over-barrier sediment fluxes for barrier island response to sea level rise (Lorenzo-Trueba and Ashton 2014; Moore et al. 2010; Wolinsky and Murray 2009), highlighting feedbacks between barrier-estuary systems. Storms are the primary driver for landward transport of littoral sediment through inlet/flood

tidal delta formation and over-wash deposition (Carruthers et al. 2013; Dillon 1970; Donnelly et al. 2006; Fitzgerald et al. 1984; Godfrey and Godfrey 1973; Leatherman 1979; Pierce 1970), but often changes to the ocean shoreline are the primary focus of storm response characterizations (Houser et al. 2007; Lentz et al. 2013; Sopkin et al. 2014; Stockdon et al. 2007). Since the magnitude of storm-related over-barrier deposition can influence future barrier island storm response (Houser et al. 2007, 2008) and can be used to predict barrier island retreat in response to sea level rise (Lorenzo-Trueba and Ashton 2014), it is important to understand spatial controls on coupled ocean shoreline losses and estuarine gains.

However, system-wide approaches to assessing storm impacts are rarely used, instead favoring approaches that separate the response of the barrier island from that of the estuary. Most assessments of the effects of hurricanes on estuaries have occurred where long-term water quality monitoring and biological data have been collected (Mallin and Corbett 2006). Therefore, the focus is often on changes to estuarine mixing (Brasseur et al. 2005; Li et al. 2007; Wilson et al. 2006) or the interaction of water column changes with estuarine biota (Mallin and Corbett 2006; Mallin et al. 1999; Peierls et al. 2003; Stevens et al. 2006; Williams et al. 2008) and not on morphological or sedimentologic changes that could influence the future behavior of the estuary and the ecosystems within it.

Of the studies identified that have addressed estuarine geomorphologic and/or sedimentologic change in response to storms, none have applied a coupled barrier-estuary approach regionally. A few studies from the Gulf of Mexico investigated the stratigraphy of existing estuarine deposits (e.g., flood tidal delta formation and over-wash deposition) and described their sedimentology (Davis et al. 1989; Israel and Ethridge 1987). However, the studies neither explored possible spatial controls on deposit location nor addressed possible connections between magnitudes of estuarine deposition and barrier island loss. Another study addressed coupled barrier-estuary geomorphologic changes in Apalachicola Bay, Florida, resulting from storms using ocean and bay shoreline profiles (Edmiston et al. 2008). However, profiles are spatially limited and may not be representative of the entire system. Another study, also in Apalachicola Bay, monitored changes to the bathymetry, sedimentology, and heavy mineral chemistry within the estuary after the passage of three hurricanes (Isphording et al. 1987). The authors concluded that the estuary experienced widespread erosion and that the sediment was deposited offshore, outside of the estuary (Isphording et al. 1987). However, there are several limitations of the study, such as coarse bathymetric resolution (>3000 m × 3000 m), lack of hydrodynamic measurements, and no measurement of sediment accumulation outside of the estuary. In order to understand spatial controls on the relationship between ocean shoreline and estuarine change, more modern observations are required.

In 2011, we began an investigation of the physical factors that influence water quality in Barnegat Bay-Little Egg Harbor estuary (referred to as Barnegat Bay throughout the text for simplicity; Fig. 1). The project intended to integrate standard techniques, such as those associated with an existing water quality monitoring network, with newer techniques, such as boat- and aircraft-based geomorphologic characterization and numerical modeling in order to develop a regional understanding of the interactions of bay geomorphology and hydrology. The project was already underway when, on 29 October 2012, Hurricane Sandy made landfall as an extratropical cyclone just south of Atlantic City, New Jersey, approximately 10 km south of the study area (Fig. 2). Updated data were collected after the storm passed, and thus, an

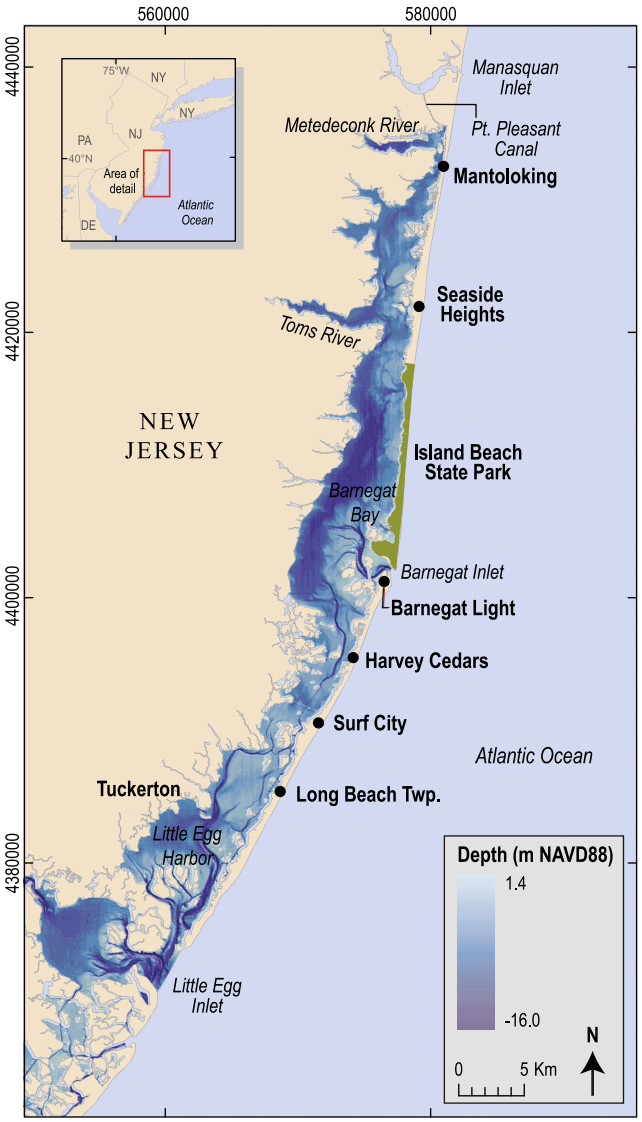

Fig. 1 Map of Barnegat Bay-Little Egg Harbor estuary with eastings and northings in UTM, zone 18N, WGS84, meters; *area in green* shows the extent of Island Beach State Park, which is relatively undeveloped in comparison to the rest of the New Jersey coast; estuarine depths from http://estuarinebathymetry.noaa.gov/finddata.html

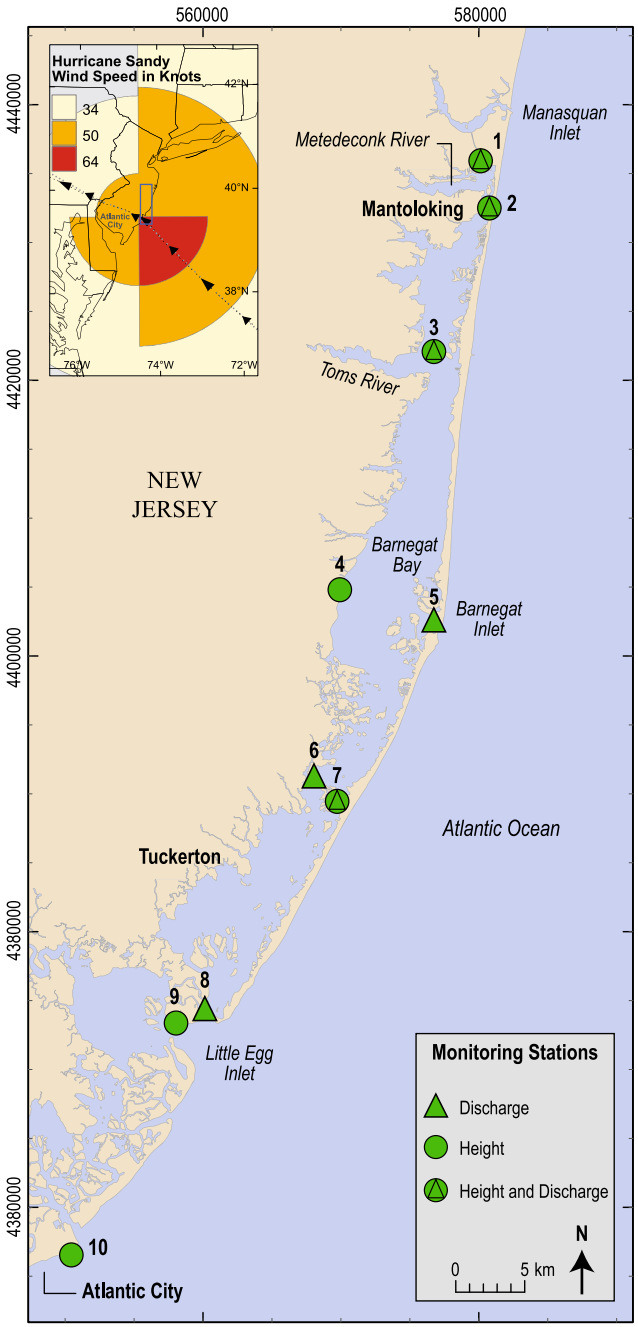

Fig. 2 *Inset* shows track of extratropical cyclone Sandy (*black line with arrows*) and wind field at landfall (*colors*); *blue box* indicates area of the larger map, which shows the locations of USGS water quality monitoring stations within Barnegat Bay and the location of the NOAA tide station near Atlantic City, New Jersey

opportunity to understand the geomorphologic and hydrologic response of a barrier island-estuary to hurricane forcing was presented.

In this paper, we use an interdisciplinary approach to understand storm-related sediment transport within the estuary and across the barrier island. We integrate geomorphic observations with numerical modeling results to understand storm-related estuarine sedimentologic changes. Hydrologic and coastal topography observations are used to provide insight into the formation of barrier island breaches that occurred during the storm. We also compare barrier island and estuary geomorphic change data to evaluate spatial controls on over-barrier sediment transport. The integration of datasets provides important insights into (1) the processes driving storm-related geomorphologic and sedimentologic changes within the coupled coastal system and (2) the spatial controls on barrier-estuary sediment exchange and may have important implications for future barrier island-estuary behavior in response to storms and sea level rise.

Study Area and Storm Characteristics

Barnegat Bay is a back-barrier estuary along the central coast of New Jersey that includes Barnegat Bay itself and Little Egg Harbor (Fig. 1). The western side of the bay is bounded by the Barnegat Bay watershed, which discharges into the estuary via two major drainages: the Metedeconk River in the north of the study area and the Toms River in the north-central portion of the estuary (Fig. 1). However, the largest source of freshwater into the northern portion of the study area is through groundwater discharge (Nicholson and Watt 1997). The eastern boundary of the estuary is comprised of a barrier spit north of Barnegat Inlet (e.g., Island Beach) and a barrier island south of the inlet (e.g., Long Beach Island). The estuary is 71 km in length and a maximum of ~7 km wide. The exchange of water between the ocean and estuary occurs only at three locations (from north to south): the Manasquan River via the man-made Point Pleasant Canal, Barnegat Inlet, and Little Egg Inlet (Fig. 1). The estuary has a mean depth of ~1 m with a network of very shallow shoals around its perimeter; shoals on the eastern side of the bay are often associated with relict or active flood tide deltas. Tides are semidiurnal, and the tidal range at Barnegat Inlet is ~1 m (Defne and Ganju 2014; Seabergh et al. 1998). However, the flood tidal shoals rapidly attenuate tidal amplitudes from 1 to 0.2 m and less north of Barnegat Inlet and from 1 to 0.2 m northward from Little Egg Inlet (Defne and Ganju 2014). Subtidal circulation is a primary driver of the spatial variability in estuarine flushing and water residence times within Barnegat Bay, with tidal rectification resulting from estuarine morphology (~75 %) and wind (~20 %) being the primary and secondary forcing mechanisms, respectively (Defne and Ganju 2014). Salinities vary widely within the bay depending on proximity to freshwater sources and inlets, but in general, mean salinities in the northern and southern portions of the study area are 18 and 25 ppt, respectively (Moser 1997).

Hurricane Sandy, an extratropical cyclone, made landfall on 29 October 2012 just north of Atlantic City, New Jersey, and approximately 10 km south of the southernmost portion of the study area (Fig. 2). This resulted in the entirety of our

survey area being in the northeast quadrant of the storm, where magnitudes of wind speed and storm surge are higher relative to other quadrants. Maximum sustained winds at landfall were 130 km/h (70 kt), but across the study area, wind speeds were predominantly ~95 km/h (50 kt) (Fig. 2, inset). Because of the large size of the storm, water levels increased along the entire east coast of the USA but the highest storm surges and most extreme inundation occurred along the coasts of New Jersey, New York, and Connecticut (Blake et al. 2013). Storm surge of 1.77 m (5.82 ft) above normal tide levels was recorded at a tide gage in Atlantic City; water levels of 1.2–1.5 m (4–5 ft) above normally dry ground level were measured along the barrier islands in the study area (Blake et al. 2013), indicating almost complete inundation of the eastern boundary of the estuary. The combination of storm surge and large storm-generated waves caused significant damage to coastal communities in the study area.

Methods

Hydrologic and Water Quality Measurements

The US Geological Survey (USGS) New Jersey Water Science Center maintains tide-level and velocity-gaging stations in Barnegat Bay that are part of state-wide networks operated in cooperation with the New Jersey Office of Emergency Management and the New Jersey Department of Environmental Protection. For this study, estuarine water levels were measured at six stations within Barnegat Bay (gages 1–4, 7, and 9); ocean water levels were derived from a National Oceanic and Atmospheric Administration (NOAA) station near Atlantic City (gage 10; Fig. 2, Table 1). Water levels at each estuarine station were measured using an Aquatrak 5000 acoustic liquid-level sensor installed on a sounding tube attached to a rigid structure over the water surface. Water levels were measured at 1-s intervals, and 3-min-average water levels were computed. Three-minute average water levels were recorded at 6-min intervals, stored using a data collection platform, and transmitted using NOAA's Geostationary Operational Environmental Satellite (GOES) to a network of computer-based stations and the Internet. Details of the New Jersey Tide Telemetry Network are described by Hoppe (2007). Meteorological information was also collected at the tidal gaging station near Barnegat Inlet (gage 5; Fig. 2).

Water velocity, a proxy for discharge, is measured at stations near the three inlets (gages 1, 5, and 8) and at stations on four bridges that cross the estuary (gages 2, 3, 6, and 7) (Fig. 2, Table 1). From these sites, discharge is calculated using a calibrated index velocity approach. Index velocity and water surface elevation were measured in a selected channel section at each station using a SonTek SL 500 Doppler flow meter side mounted on a bracket attached to a bridge support, bulkhead, or other rigid structures. Measured velocity and water surface elevation data were used with the index velocity method (Ruhl and Simpson 2005) to compute continuous records of flow through the bay section. The measured flow was recorded at 6-min intervals. The application of the method to estuarine environments by the USGS is described by Gotvald and Oberg (2009).

Turbidity and salinity measurements were also measured during the storm at a continuous water quality monitoring station located on the bridge that crosses the estuary near the town of Mantoloking, in the northern part of the study area (gage 2; Fig. 2). Measurements were made by pumping water from the bay into an instrument shelter situated on the bridge. Water was pumped from the bay at a depth of 2.14 m (7 ft) below mean water (or ~40 cm above the bed) through a 2.54-cm (1-in.) PVC pipe into a 3.79-L (10-gal.) polyethylene tank every 30 min. Stagnant water in the intake pipe was flushed for 3 min and discharged prior to filling the tank. Specific conductance of unfiltered water was then measured using a YSI 6920 data logger and a YSI 6560 sensor and recoded as microsiemens per centimeter at 25 °C. Turbidity of unfiltered water was measured using a YSI 6136 sensor using monochrome near-infrared LED light (780–900 nm, detection angle 90° + −2.5°) and recorded as formazin nephelometric units (FNU). Salinity was calculated from specific conductance and temperature measurements.

Geophysical and Sedimentologic Measurements

Boat-based geophysical and sedimentological data were collected in water depths greater than 1.5 m during four cruises: November 2011, March 2012, March 2013, and September 2013; the first two surveys occurred before Hurricane Sandy made landfall, and the last two occurred after the storm (Fig. 3). All of these data are published with metadata in Andrews et al. (2015), and thorough descriptions of data acquisition and processing methodologies are described therein. Techniques specific to the analysis are summarized here. Swath bathymetry, side scan sonar, and high-resolution seismic reflection data were collected simultaneously and spatially referenced in real time using RTK-GPS, though only the bathymetry is pertinent to this analysis. More than 2000 line-km of data was collected, covering approximately 30 % of the area of the bay or ~100 km^2. Because of the shallow nature of the bay, track lines had a spacing of 50 m to ensure 100 % coverage with side scan sonar, except within the Mantoloking embayment where 100 % bathymetric coverage was achieved and in the inlet channels where line spacing varied depending on the width of the channel. Only the Mantoloking embayment was surveyed before and after the storm in November 2011 and March 2013, respectively. Bathymetry was collected using a SwathPlus-H interferometric sonar using a frequency

Table 1 Water level gage information

Gage no.	Geographic location	Station ID	Longitude	Latitude	Measurements
1	Point Pleasant Canal at Point Pleasant, NJ	1408043	74° 03′ 34″	40° 04′ 15″	Water level and discharge
2	Barnegat Bay at Mantoloking	1408167	74° 03′ 08″	40° 02′ 24″	Water level and discharge
3	Barnegat Bay at Rt 37 bridge near Bay Shore, NJ	1408205	74° 06′ 09″	39° 56′ 46″	Water level and discharge
4	Barnegat Bay at Waretown, NJ	1409110	74° 10′ 55″	39° 47′ 28″	Water level
5	Barnegat Inlet at Barnegat Light, NJ	1409147	74° 06′ 15″	39° 45′ 49″	Water level and discharge
6	Manahawkin Bay at Rt 72 bridge near Ship Bottom, NJ	140914550	74° 12′ 25″	39° 39′ 48″	Water level and discharge
7	East Thorofare at Ship Bottom, NJ	1409146	74° 11′ 09″	39° 39′ 14″	Water level and discharge
8	Little Egg Inlet near Beach Haven Heights, NJ	1409334	74° 18′ 05″	39° 30′ 42″	Water level and discharge
9	Little Egg Inlet near Tuckerton, NJ	1409335	74° 19′ 29″	39° 30′ 32″	Water level
10	Atlantic City, NJ (Atlantic Ocean)	NOAA 8534720	74° 25′ 5″	39° 21′ 24″	Ocean water level

of 468 kHz, and soundings were corrected for vessel motion in real time using a Coda Octopus F-190 motion reference unit mounted directly above the transducers. Sound velocity profiles were collected as needed or every 2 h to reduce depth errors associated with signal refraction.

Geophysical data were validated using the USGS SEABed Observing and Sampling System (SEABOSS), which collects bottom photographs, bottom video, and sediment samples (Valentine et al. 2000). Sediment sampling surveys followed the last three geophysical surveys, and sampling locations were chosen based on the backscatter, bathymetry, and seismic data. During the post-storm cruise in March 2013, 26 sites that had been sampled prior to Hurricane Sandy in March 2012 were revisited (Fig. 3). A Van Veen sediment grab collected 0.1-m^2 samples of undisturbed seafloor, the surface of which was sampled with a 2-cm scoop. Samples were wet sieved through a 0.62-mm sieve to separate fine and coarse fractions. Coarse fractions (sand and gravel) were oven-dried, weighed, and dry sieved, while the fine fractions (silt and clay) were analyzed using a Coulter Counter Multisizer 3; this allowed for determination of grain sizes from −5 to 11 phi. Sediment classification and frequency percentages were calculated using GSSTAT software (Poppe et al. 2004), which is based on methods of Folk (1974) and Collias et al. (1963).

Since the majority of Barnegat Bay is comprised of shallows less than 1.5 m in depth, mapping of the bay could not rely on boat-based acoustics alone. Instead, the shoals and flood tidal deltas in the estuary were mapped using the USGS Experimental Advanced Airborne Research Lidar (EAARL-B), a new generation of the EAARL system that acquires topographic and bathymetric data using an aircraft-mounted laser (Wright et al. 2014a). Fortuitously, a survey of the bay was already underway well before Hurricane Sandy was predicted to affect New Jersey and took place over 4 days between 18 and 26 October 2012. Just prior to landfall, the EAARL-B system was redirected to respond to pre-storm assessments of the Atlantic Coast as Sandy developed. All of the bay, with the exception of the western portions of Little Egg Harbor and Barnegat Bay, was mapped using EAARL-B prior to Sandy (Fig. 4, left panel). Details of processing and acquisition for these surveys can be found in Wright et al. (2014a). After the storm, the bay was very turbid, limiting the penetration of the laser. Windows of improved water clarity were targeted, and therefore, nine post-storm EAARL-B surveys occurred between 1 November 2012 and 10 January 2013. Unfortunately, post-storm coverage of the bay was significantly limited by water clarity (Fig. 4, right panel). Details of the acquisition and processing methods can be found in Wright et al. (2014b). EAARL-B was also used to map the New Jersey coastline 3 days prior to landfall on 26 October and covered the region from Cape May Point to Sandy Hook. The post-storm response of the coastline was surveyed between 1 and 5 November using the same EAARL-B system. Methods for calculating coastal change for the entire Atlantic Coast resulting from Hurricane Sandy are reported in Sopkin et al. (2014).

Further spatial analysis was conducted for the study area north of Barnegat Inlet because of the distinct difference in land use that occurs along that portion of the coast (Fig. 1). A quasi-shore-parallel baseline was established seaward of the ocean shoreline. Baseline-perpendicular transects were cast from the baseline to just beyond the mainland shoreline so that they crossed both the barrier island and the estuary. Transects were spaced every 50 m in the alongshore direction and were used to characterize the cross-estuary and island geomorphology (e.g., width, cross-sectional area, and maximum depth). Transects were also used to establish alongshore bins, which were used to summarize and compare coastal and estuarine changes (e.g., beach and dune volume changes, and estuarine volume changes).

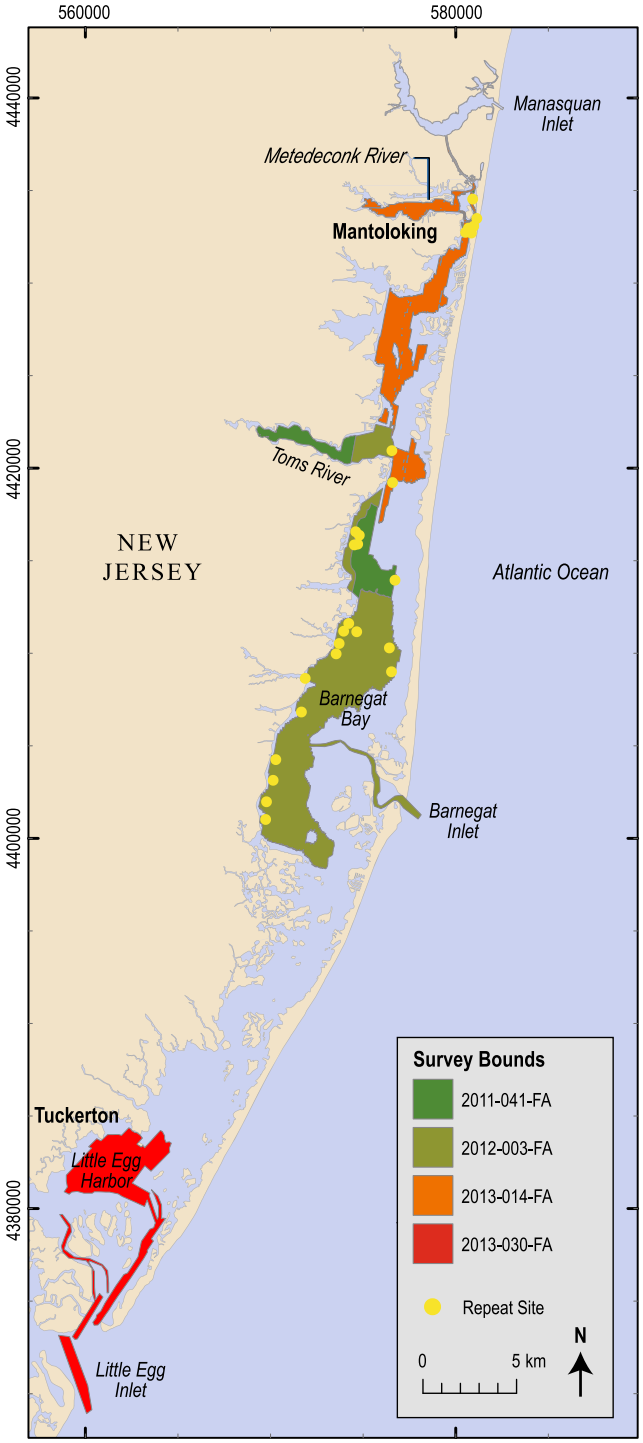

Fig. 3 Map of geophysical survey coverage collected over 2 years; *areas in green* were surveyed prior to Sandy, and *areas in red and orange* were surveyed after the storm; *yellow circles* indicate locations of 26 sediment sampling sites visited before and after the storm

Hydrodynamic and Sediment Transport Modeling

Hydrodynamics and sediment transport were simulated with a modified version of the Barnegat Bay model described by Defne and Ganju (2014); in this case, we activated the wave (SWAN) and sediment transport (CSTM) components of the COAWST modeling system (Warner et al. 2010) for the period 1 October 2012–25 November 2012. The bathymetry and topography within the model domain were derived from a terrain model that integrated acoustic bathymetry and lidar bathymetry from this study and lidar topography from the state of New Jersey (see Andrews et al. 2015). The sediment bed was initialized with an equal distribution of three classes of sediment representing silt (50 μm), fine sand (100 μm), and medium sand (250 μm). The time series of maximum combined wind-current shear stress, using the formulation of Madsen (1994), was extracted from the period representing the influence of the storm (28 October 2012–2 November 2012), and time-averaged to yield a spatial map of mean combined stress over the entire model domain; vertical changes in bed elevation from the same period were extracted as well.

Results

Characterizing the Estuarine and Coastal Impact of Hurricane Sandy

Changes in Estuarine Hydrology

Hydrologic data demonstrate a strong relationship between estuarine water levels and storm-related wind direction. During the approach of the storm, a northerly wind direction predominated over Barnegat Bay resulting from counterclockwise storm rotation (Fig. 5(a)). The wind shifted to a southerly direction after the storm made landfall (Fig. 5(a)). Because Barnegat Bay is very shallow and is oriented in a north-to-south direction, these changes in wind direction drove significant water level changes. Water levels at the three southern stations (4, 7, and 9) all started to rise ahead of the storm, with a tidal signature similar to the ocean tides measured near Atlantic City (gage 10; Fig. 5(b)). The three northern stations (1–3) had relatively normal water levels until landfall when the wind shifted from north to south; at that time, water levels increased rapidly in a matter of hours (Fig. 5(b)). The most significant increase was measured at gage 2 near Mantoloking, where water levels rose 2.48 m (−0.38 to 2.11 m, NAVD88) in 8.2 h. This is a significant departure from normal tidal conditions, where water levels in the interior part of the estuary range from −0.30 to 0.3 m (NAVD88).

The wind-driven ebbing and rapid flooding described above are also evident in the discharge data from gage 1, which shows ocean-to-bay (negative) flow directions prior to landfall followed by persistent bay-to-ocean (positive) flow directions shortly after landfall (Fig. 5(c)). Bridge station data also support storm-driven ebbing and rapid flooding, with two of the gages (3 and 7) recording rapid northerly discharges

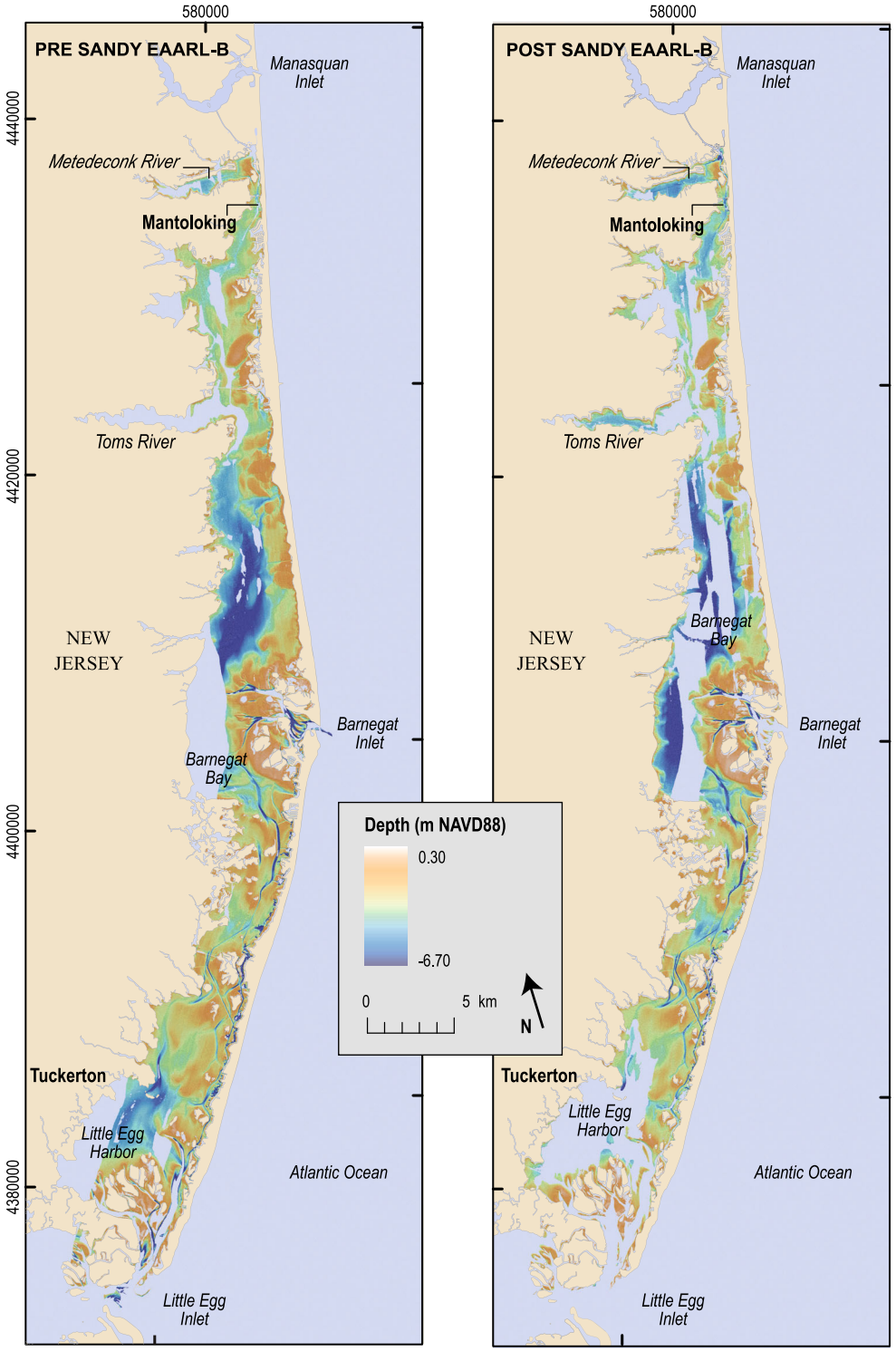

Fig. 4 Maps of EAARL-B bathymetric lidar data collected before (*left panel*) and after (*right panel*) Hurricane Sandy; post-storm data acquisition was limited by poor water clarity

(negative) coincident with the shift in wind direction and rapid flooding of the northern parts of the bay (Fig. 5(c)). It is interesting to note that the magnitude of post-landfall southerly discharge (positive) is much smaller than the magnitude of northerly discharge (negative) during the height of the storm; this suggests that elevated water levels persisted in the northern part of the bay beyond 31 October.

Turbidity and salinity data recorded at the station near Mantoloking show coincident increases in turbidity and salinity as the storm approached (Fig. 6). Turbidity and salinity

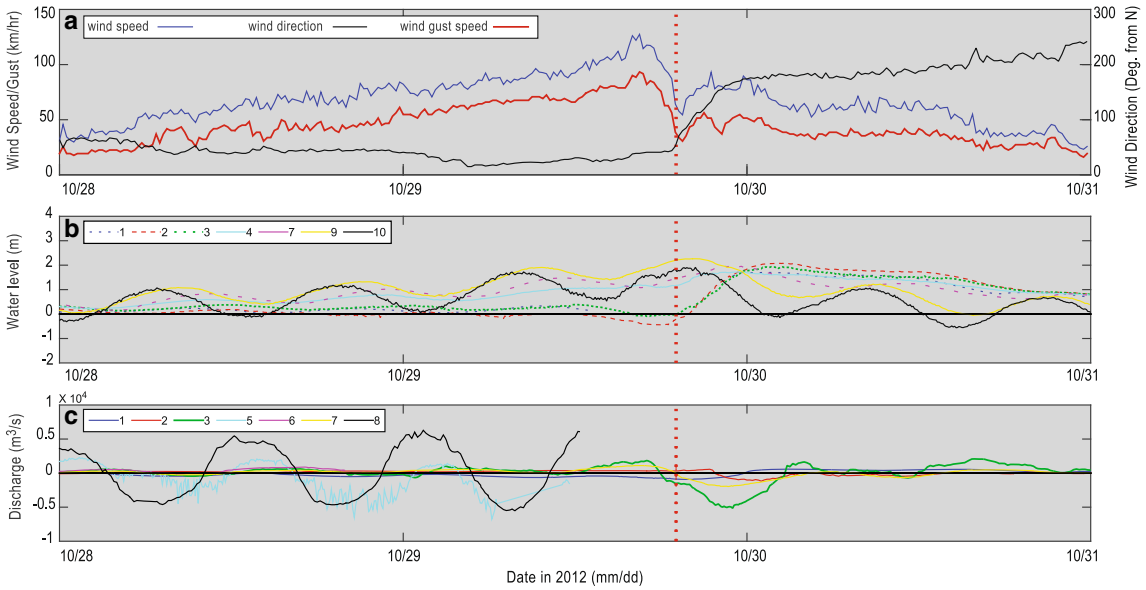

Fig. 5 *a* Meteorological data collected at Barnegat Light during the approach, landfall, and passing of Hurricane Sandy; *vertical dashed red line* indicates landfall and the beginning of a change in wind direction. *b* Changes in estuarine and ocean (gage 10, *black*) water levels during the storm. *c* Changes in estuarine discharge during the storm

measurements from a water level and turbidity station in the bay and west of Barnegat Inlet were compared to the results from Mantoloking. Prior to landfall, peaks in turbidity and salinity are lagged between the two stations, appearing first at Barnegat Inlet and then at Mantoloking. Furthermore, the magnitude of the turbidity increase is very similar between the two stations. These observations suggest that the pre-landfall peaks in salinity and turbidity measured at Mantoloking result from semidiurnal tidal advection of sediment and slightly more saline water from south to north. Shortly after landfall, a large peak in turbidity (~440 FNU) is measured at Mantoloking (Fig. 6). Unlike previous increases, this one was not preceded by an increase in turbidity at the station near Barnegat Inlet. Also, this value marks a clear departure from values observed regularly (<10 FNU), during the spring phytoplankton bloom (5–15 FNU), during seasonal wind or rainfall events (~100 FNU), and prior to landfall (~100–150 FNU). Elevated turbidity and salinity just after landfall are likely related to a breach in the barrier spit adjacent to the bridge in Mantoloking that occurred during the storm (described in the next section). The breach would have entrained large volumes of sediment and allowed higher salinity ocean

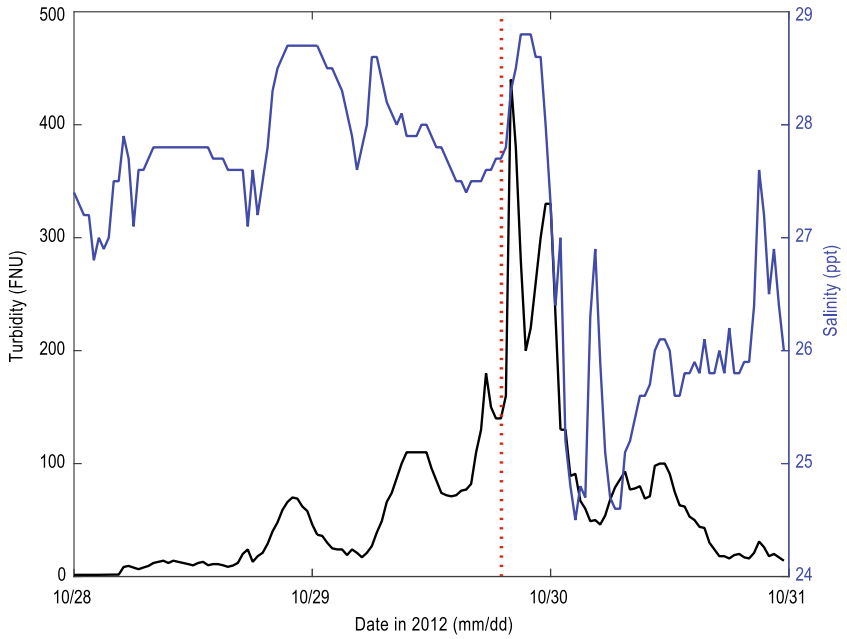

Fig. 6 Changes and turbidity (*left y-axis*, *black*) and salinity (*right y-axis*, *blue*) near Mantoloking during the storm; *red dashed line* indicates storm landfall and beginning of change in wind direction from north to south

water to enter the bay. The marked decrease in salinity is indicative of the rapid flooding of the northern part of Barnegat bay with fresher water after the shift in wind direction, while the slow increase in salinity over 30 October suggests mixing of ocean and fresher water near the breach.

Storm Effects on Coastal-Estuarine Geomorphology and Sedimentology

Some of the most significant changes to the geomorphology of the coast were observed on the barrier spit and barrier island east of the bay. This is not surprising considering that estimated 10 % exceedance total high water levels (surge + runup) were almost always greater than the pre-Sandy elevation of the dune toe and often greater than the elevation of the dune crest (Fig. 7). Averaged across the study area, the barrier shoreline retreated by 12 m during the storm. However, the response varied considerably along the coast and approximately 46 % of the shoreline experienced greater than average shoreline retreat (Fig. 8(a)). Dune elevations and beach volumes almost always decreased across the study area (Fig. 8(b, c)). The highest number of zero or near-zero changes in dune height was recorded in the relatively undeveloped area of Island Beach State Park (IBSP) which comprises the area from Barnegat Inlet to ~15 km north (Fig. 8(b)). The largest decrease in dune height was observed near Mantoloking and coincided with a large breach in the barrier spit (Fig. 8(b); see aerial photos in Fig. 9).

Storm-related estuarine bathymetric changes, including those associated with both breaches that occurred near Mantoloking, were assessed using a combination of acoustic and lidar bathymetry before and after the storm. Differencing the pre- and post-storm bathymetry for the entire estuary (where there was overlap) demonstrates that the storm resulted in ~250 km^3 of deposition and ~50 km^3 of erosion within the bay, amounting to ~200 km^3 net storm-related accretion (measurable change ± 35 cm). Measurable change was not widespread, but rather very localized. In the Mantoloking embayment, the change almost exclusively resulted from breaches in the barrier island (Fig. 9). The combined volume of deposited sediment associated with the breaches was ~19,100 m^3, ~80 %

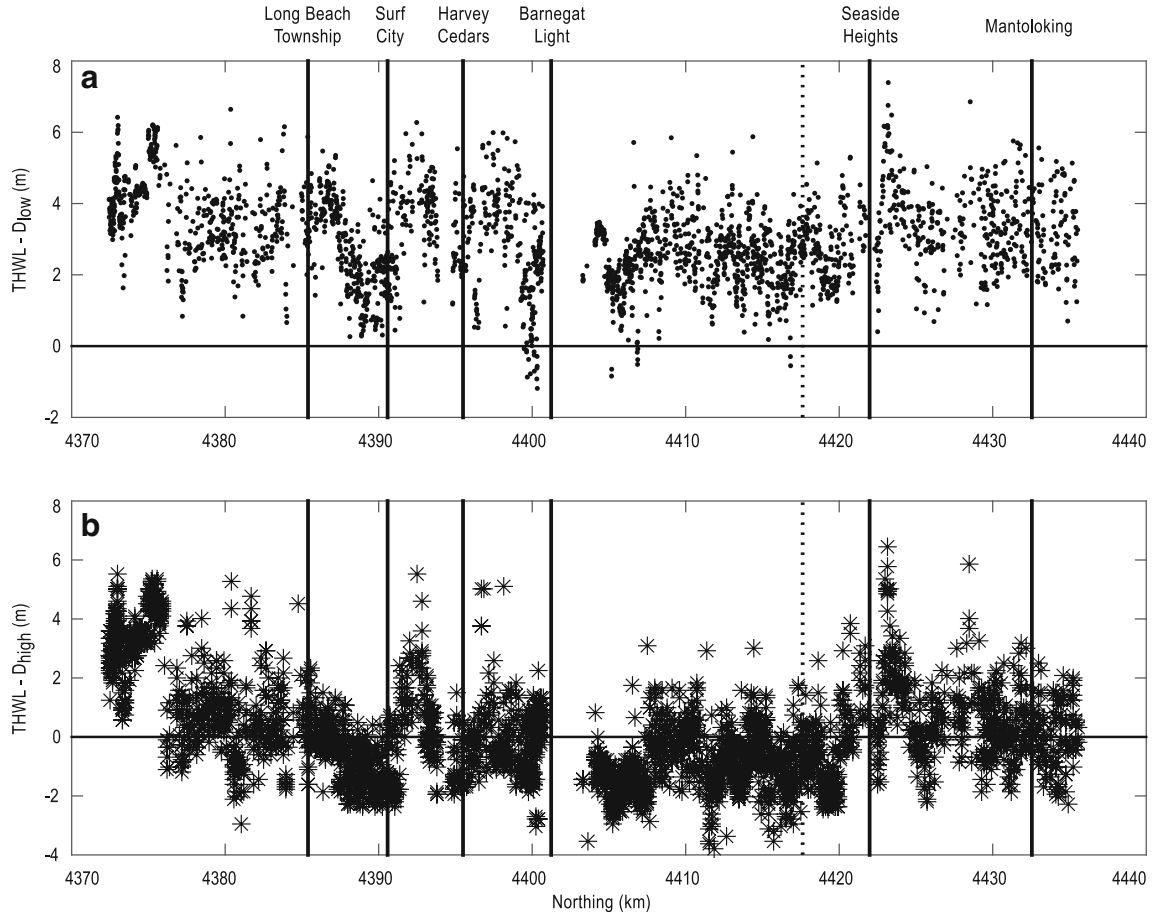

Fig. 7 Alongshore variability in the difference between estimated 10 % exceedance total high water level (*THWL*) and the elevation of the dune toe (D_{low}, *a*) and dune crest (D_{high}, *b*) for the entire study area; *solid vertical lines* indicate the location of geographic landmarks along the coast; *dashed vertical line* indicates the northern boundary of Island Beach State Park, south (left) of which is relatively undeveloped barrier island

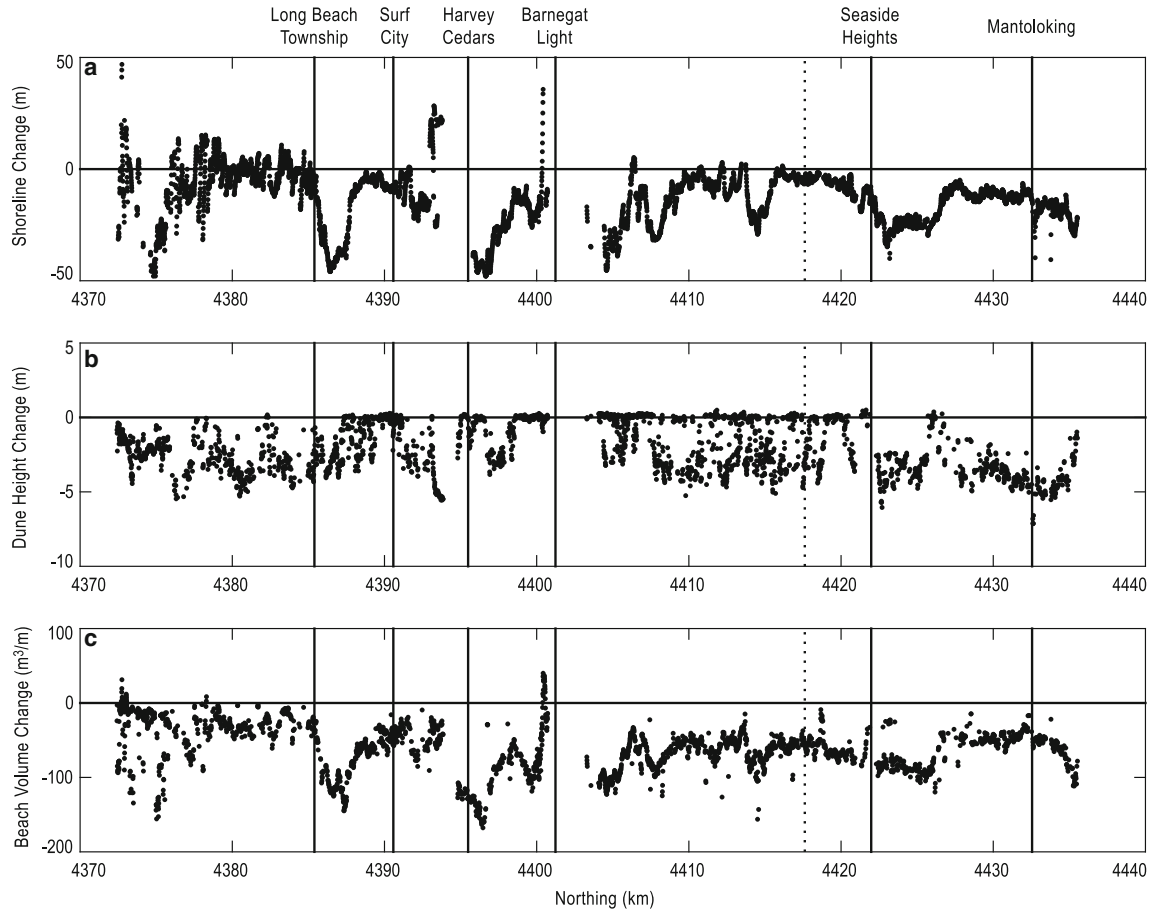

Fig. 8 Alongshore variability in shoreline change (*a*), dune elevation change (*b*), and beach volume change (*c*) for the entire study area; *solid vertical lines* indicate the location of geographic landmarks along the coast; *dashed vertical line* indicates the northern boundary of Island Beach State Park, south (*left*) of which is relatively undeveloped barrier island

of which was associated with the larger, southern breach. Breach deposition accounts for 10 % of the net change measured for the entire estuary.

Spatial variability in estuarine changes was explored north of Barnegat Inlet and showed very little net change (Fig. 10). Large volumes deposited generally corresponded to large volumes eroded. This suggests that in general, Sandy caused local changes in estuary morphology (e.g., bedform migration and channel migration) rather than significantly altering the regional geomorphology of the estuary. Localized gains and losses were observed around the perimeters of the bay, along the back-barrier and mainland shorelines, and across the flood tidal shoals of Barnegat Inlet.

A further look at the data shows that the location of storm-related estuarine deposition is spatially related to two factors: (1) estuarine depth and (2) barrier island land use. Figure 11a, b shows the distribution of distances from the back-barrier shoreline to the maximum estuarine depth for developed and undeveloped portions of the barrier island, respectively. For developed barrier island, 31 % of the deepest depths are within 0.5 km of the back-barrier shoreline whereas only 4 % of the deepest depths are within the same distance for undeveloped barrier. These data demonstrate differences in back-barrier-adjacent estuarine geomorphology between developed and undeveloped coastlines. Figure 11c, d shows the distribution of distances from the back-barrier shoreline to the location of maximum measured estuarine deposition for developed and undeveloped barrier islands, respectively. Almost 60 % of storm-related estuarine deposition occurred within 0.5 km of the developed back-barrier shoreline, while less than 20 % occurred within 0.5 km of the undeveloped back-barrier shoreline. These data suggest that storm-related estuarine deposition is more likely to occur directly adjacent to developed back-barrier shoreline. The combination of these data demonstrates that for developed barriers, estuarine depth and its proximity to the back-barrier shoreline may be a primary control on the location of storm-related deposition. For undeveloped barriers, maximum estuarine deposition is sometimes found adjacent to the back-barrier shoreline but is largely independent of back-barrier depth.

Finally, comparisons of pre- and post-Sandy surface sediment samples show that the majority of sites became better

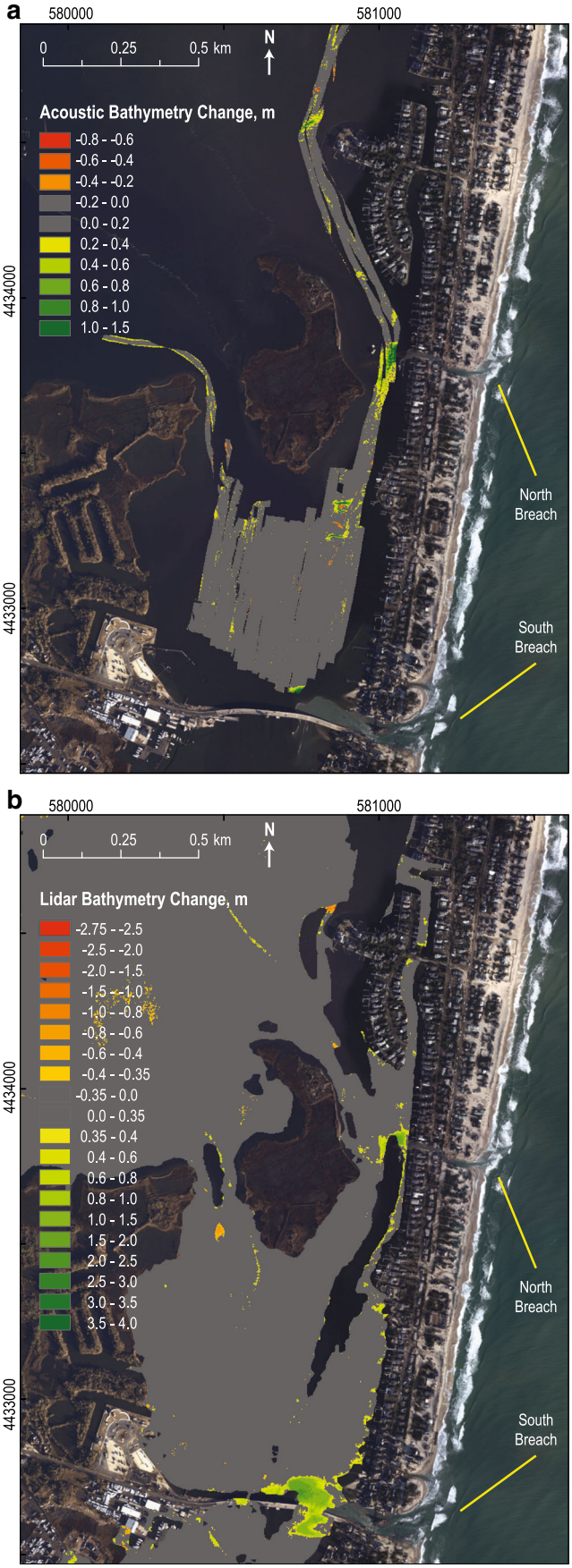

◀ **Fig. 9** Acoustic (**a**) and lidar (**b**) estuarine bathymetric change associated with extratropical cyclone Sandy within the Mantoloking embayment; *red and orange colors* indicate erosion, *yellow and green colors* indicate deposition, and *gray values* indicate no change or change below the resolution of the respective instruments; aerial photographs from http://storms.ngs.noaa.gov/storms/sandy/

sorted and coarser as a result of the storm. Because of the lack of post-storm lidar coverage at many of the sediment sampling sites, it was difficult to determine if the improved sorting and coarsening of the seabed were related to the deposition of coarse material in the estuary or the erosion of finer material from the seabed. To determine the cause for the changes, we compared the sedimentologic data to model-simulated bed shear stress. One site was removed from the regression since it was associated with a deposit from one of the breaches and breaching was not simulated in the model (Fig. 12). Sorting change (more negative = more sorted) is negatively correlated with shear stress, indicating that better sorting in post-storm samples is associated with higher bed shear stress (Fig. 12a). Skewness and bed shear stress were positively correlated (Fig. 12b), indicating a coarsening of the post-storm sample with increased bed shear stress. These results suggest winnowing as the mechanism for surficial sediment changes rather than deposition of coarser material.

Exploring Spatial Controls on Barrier Island-Estuary Connectivity

Comparisons of the measured barrier island volume loss (e.g., the bin sum of beach and dune volume changes) and estuarine volume gain (e.g., cumulative estuarine deposition divided by the alongshore bin width, or 50 m, in m^3/m) were used to explore spatial controls on barrier-estuary connectivity, defined as a sediment exchange between barrier island and estuary. No linear relationship was found between barrier island losses and estuarine volume gains for the study area (Fig. 13). This is likely due to the spatially discrete nature of the estuarine deposits (Fig. 10c) relative to the somewhat more uniform response of the beach and dunes (Fig. 8b, c). However, summary statistics do reveal some spatial differences in island-estuary connectivity related to barrier island land use and width (Table 2). On average for the developed shoreline, ~30 % more sediment accumulation was measured in the estuary relative to undeveloped shoreline despite greater barrier island losses in the undeveloped region (Table 2). Furthermore, despite similar barrier island losses, ~30 % more estuarine accumulation was observed in areas where island width was less than the regional average (634 m) compared to areas where width exceeded the regional average (Table 2). These results demonstrate the role of barrier island land use and width in barrier-estuary connectivity.

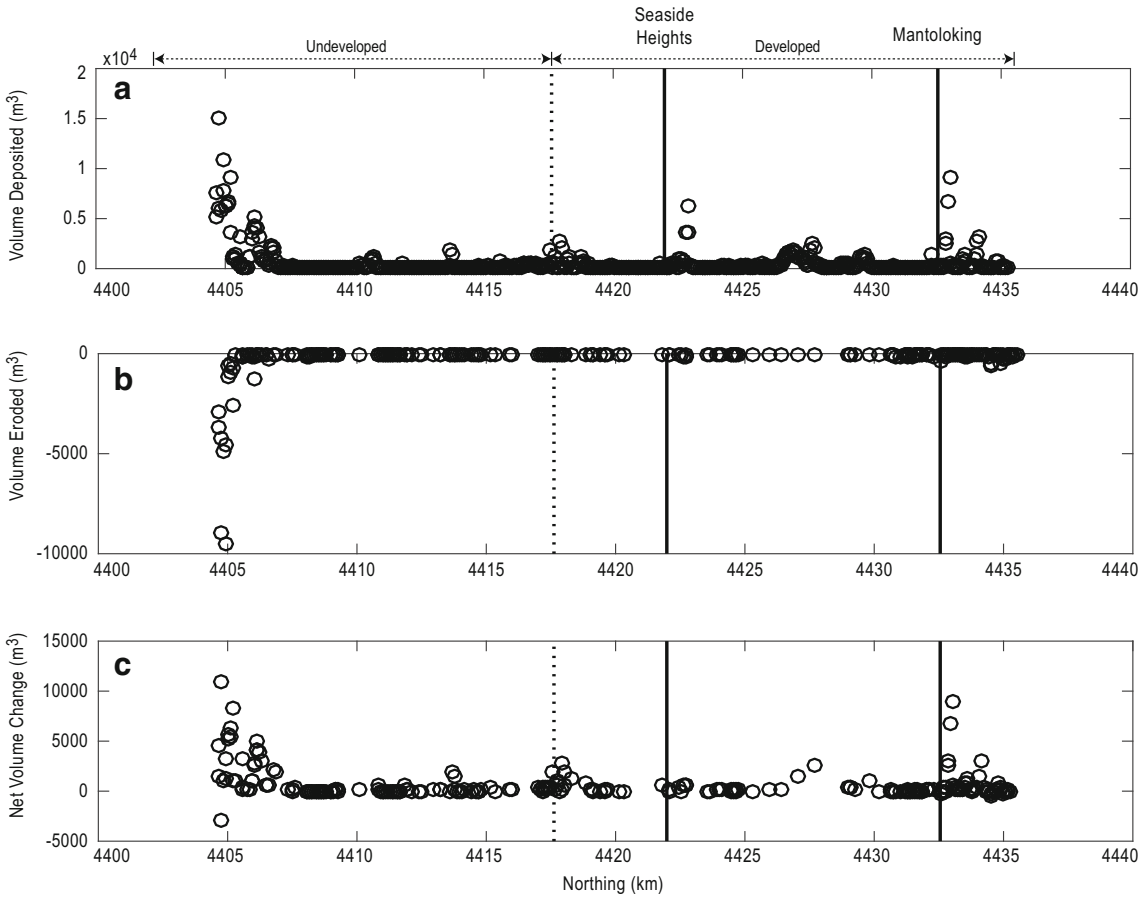

Fig. 10 Alongshore variability in volume of estuarine deposition (*a*), estuarine erosion (*b*), and net change (*c*) for the portion of coast north of Barnegat Inlet; *solid vertical lines* indicate the location of geographic landmarks; *dashed vertical line* indicates the distinct transition between relatively undeveloped coastline associated with Island Beach State Park to the south (*left*) and heavily developed coastline to the north (*right*)

Discussion

Sandy ocean shorelines have long been the focus of storm response investigations. Back-barrier morphology and sedimentology have only recently been recognized as a significant influence on barrier evolution in response to storms and sea level rise (Hawkes and Horton 2012; Lorenzo-Trueba and Ashton 2014; Moore et al. 2010; Shaw et al. 2015; Wolinsky and Murray 2009), and the mechanisms of estuarine storm response are poorly understood. Below, we discuss our results in the context of storm-related sediment transport in order to improve understanding of mechanisms of and spatial controls on storm-related estuarine geomorphic change and sediment transport between barrier islands and estuaries.

Estuarine Geomorphologic and Sedimentologic Storm Response

Morphologic Changes

The scope of estuarine geomorphologic data collected and the integration of those data with coastal change data and model simulations allows for a coupled assessment of barrier island-estuary geomorphic change resulting from an extreme storm. As might be expected given conceptual models of barrier island rollover (Leatherman 1979; McBride et al. 1995), there was a net addition of sediment (~200,000 m^3) into the estuary resulting from Hurricane Sandy. However, estuarine gains were not spread uniformly along the back-barrier shoreline, but rather in spatially discrete deposits. This spatial variability in estuarine deposition is important for two reasons. First, it

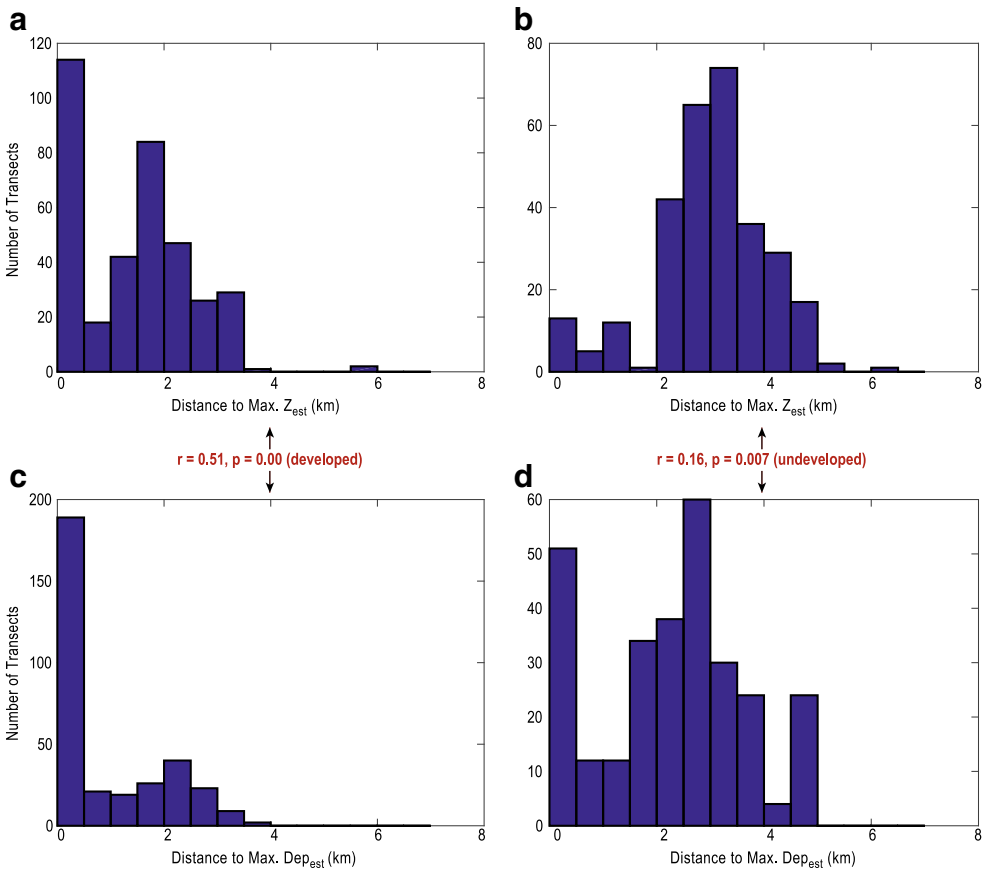

Fig. 11 Comparisons between estuarine morphology (maximum estuarine depth) and distance from the back-barrier shoreline relationship for developed (**a**) and undeveloped (**b**) barrier island locations; comparisons between storm-related deposition (maximum estuarine deposition) and distance from the back-barrier shoreline for developed (**c**) and undeveloped (**d**) barrier island locations; note that the correlation between morphology and storm-related deposition is higher for developed areas

demonstrates that barrier-to-estuary fluxes are not alongshore uniform and, therefore, approaches that consider barrier-estuary change along profiles may be significantly under- or over-estimating regional landward sediment flux. Second, the alongshore variable landward sediment flux has implications for future barrier island evolution. Increased estuarine deposition may allow the barrier to keep up with sea level rise, while lower fluxes may result in drowning (Lorenzo-Trueba and Ashton 2014). However, more information is needed about how storm-related transport is integrated over long time scales before model predictions of barrier island response to sea level rise can be validated.

Relationships were found between barrier island land use and estuarine morphology and the location and magnitude of storm-related estuarine deposition. First, it was much more common for maximum estuarine depth to be within 0.5 km of the back-barrier shoreline for developed portions of the barrier (~31 %) than for undeveloped areas (~4 %). This observation is likely related to extensive bulkheads that line the eastern estuarine shoreline of Barnegat Bay (~45 %; Kennish 2001), which were put in place to maintain navigable (e.g., deeper) water depths dredged adjacent to the back-barrier shoreline. Differences in estuary storm response were also noted for location of maximum storm-related deposition, with 60 % occurring within 0.5 km of developed back-barrier shoreline compared to only 20 % for undeveloped barrier. This may not be surprising, considering that streets and beach access points along the barrier can serve to direct flow, thereby increasing transport efficiency (Carruthers et al. 2013; Morton 2002). These results might appear to suggest that developed barriers are better at moving sediment from barrier to estuary. However, collocation of that deposition with dredged channels suggests that sediment is unlikely to remain in place to support future barrier island evolution, effectively resulting in zero over-barrier sediment flux. With no addition of sediment to the back-barrier environment and with increased rates of sea level rise, barrier islands cannot maintain their elevation and width and drown (Lorenzo-Trueba and Ashton 2014). Between alongshore variable estuarine deposition and coastal sediment management practices, it is clear that storm-related over-barrier transport is a highly complex process and that a new conceptual model for barrier rollover that accounts for

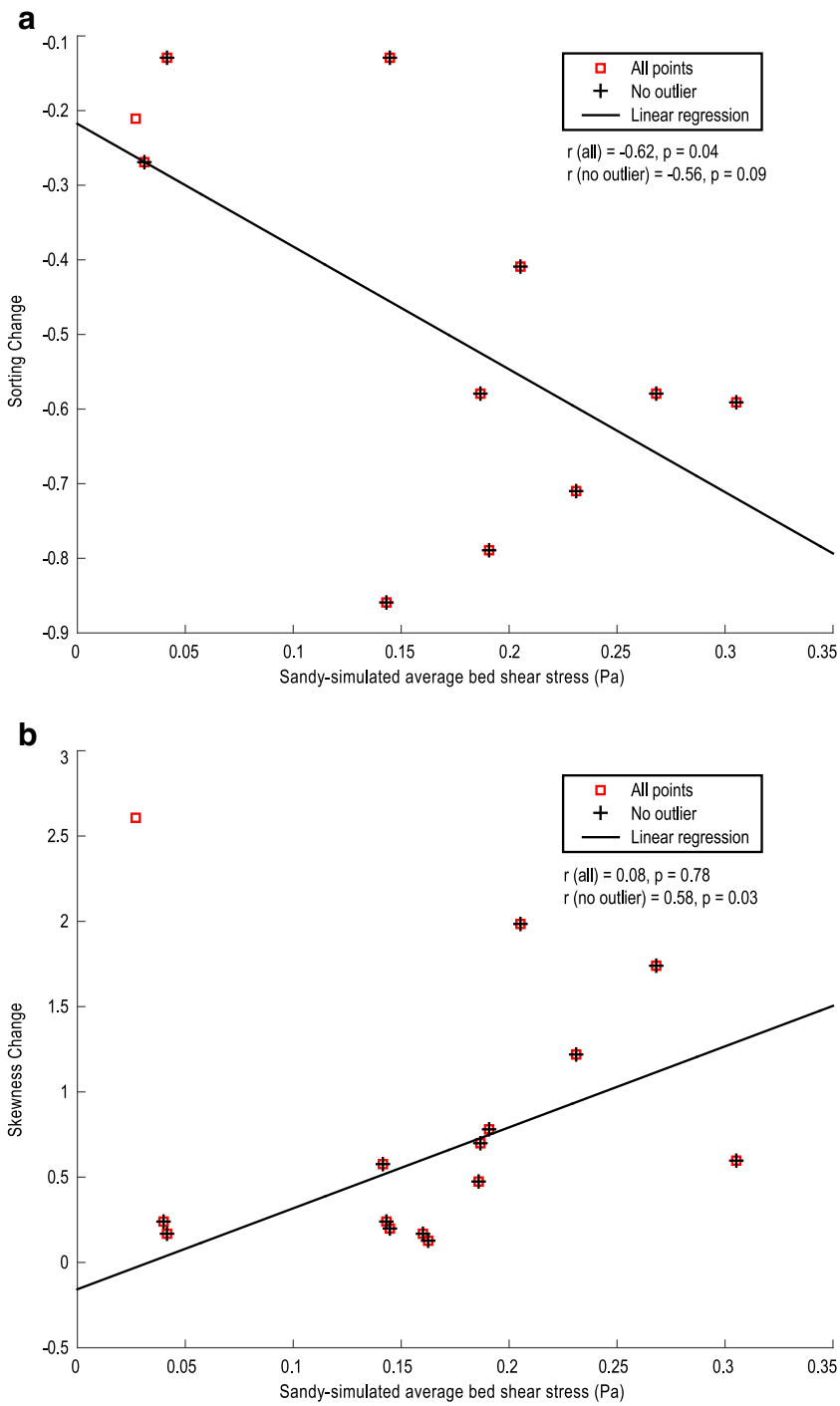

Fig. 12 Comparisons between measured sorting change (**a**) and skewness change (**b**) and shear stress values derived from model-simulated conditions during Sandy

alongshore variability and coastal and estuarine land use is needed.

Sedimentologic Changes

Comparison of the sediment changes to model-simulated bed shear stress during Sandy shows a strong correlation between increased shear stress and improved sorting and coarsening. This indicates that winnowing was the process driving storm-related sediment change in Barnegat Bay, which could influence the sedimentology of existing (pre-Sandy) estuarine storm deposits and the stratigraphic interpretation of their origin (Davis et al. 1989). Estuarine currents associated with the passage of three hurricanes near Apalachicola Bay, Florida, were identified as the mechanism for estuarine sedimentologic change, similar to our results (Isphording et al. 1987). However, that study concluded that the sediment changes were the result of widespread estuarine erosion, resulting in

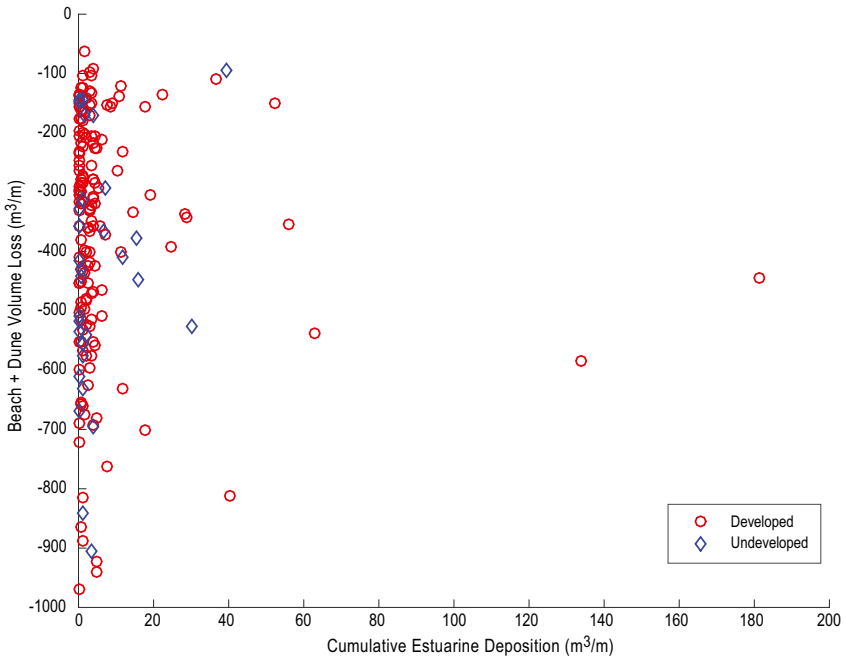

Fig. 13 Comparison of measured barrier island sediment loss to volume of estuarine deposition for undeveloped (*blue diamonds*) and developed (*red circles*) locations

the export of sediment out of the estuary and the exposure of slightly older sediments within the estuary. Our data do not show any evidence of sediment export out of the estuary (net accumulation was observed), and because the sediment changes were accompanied by little to no measureable change in depth, we can also rule out widespread estuarine erosion. It has been suggested that storm characteristics, such as intensity, proximity to study sites, and duration, can influence storm response (Mallin and Corbett 2006; Morton 2002). This does not appear to be true for the comparison between Apalachicola and Barnegat bays. Though three storms impacted Apalachicola Bay, the closest track was about 50 miles west (Isphording et al. 1987). The proximity of Sandy's landfall to Barnegat Bay and the unique and almost perpendicular track of the storm (Hall and Sobel 2013) would suggest that our study site experienced far more intense conditions than Apalachicola Bay and yet little widespread morphologic and sedimentologic change was observed. The primary difference between this study and the Apalachicola study is the resolution of the observational datasets; in Apalachicola Bay, the change was measured over an area greater than 3000 m × 3000 m whereas the resolution of the estuarine bathymetric data from Barnegat was 3 orders of magnitude less (~3 m × 3 m). Though more storm-related estuarine morphologic and sedimentologic change data are needed to further understand storm impact on estuaries, we believe that the results from Apalachicola are the exception rather than the rule and that future estuarine storm response investigations will show results similar to those from Barnegat Bay.

Barrier Island Breaching: Links Between Hydrologic Response and Estuary-Island Geomorphology

One mechanism of getting sediment into back-barrier environments during storms is through barrier island breaches (Dillon 1970; Donnelly et al. 2006; Fitzgerald et al. 1984; Pierce 1970). Therefore, we explored the mechanisms responsible for Sandy-related breach formation and the magnitude of breach deposition at the study site. Two breaches in the barrier spit occurred near Mantoloking, New Jersey, despite Hurricane Sandy landfall occurring approximately 80 km to the south. The relationship between dune height and surge elevation is often cited as a primary control on barrier island response to storms (Houser et al. 2008; Morton 2002; Sallenger 2000; Thieler and Young 1991). However, estimated total high water levels (surge + runup; total high water level (THWL)) above the dune crest were higher along other parts of the coast than they were at the southern breach location, indicating some other causes behind breach formation.

Our data suggest that the hydrostatic head between the estuary and ocean and island-estuary width may have also influenced the breach formation near Mantoloking. Water level data show negative estuarine water levels at the Mantoloking station coupled with a peak in ocean water levels at landfall. This resulted in an ocean-to-bay water level difference of at least 2 m (note that ocean water levels were recorded at Atlantic City, 80 km south of the breach). It is right after this that peaks in turbidity and salinity were recorded at Mantoloking, indicating that

Table 2 Comparison of measured barrier island sediment losses and estuarine gains

	Barrier island loss (m^3/m, mean (std))	Estuarine gain (m^3/m, mean (std))	Percent transported to estuary	Percent transported elsewhere
All	–383.78 (±203.43)	6.53 (±16.78)	1.70	98.30
Developed shoreline	–372.44 (±202.17)	6.82 (±17.67)	1.83	98.17
Undeveloped shoreline	–442.67 (±203.03)	4.67 (±8.92)	1.06	98.94
Island width > average	–380.92 (±216.53)	4.91 (±8.90)	1.29	98.71
Island width < average	–385.69 (±195.12)	7.87 (±21.07)	2.04	97.96

the island had been breached. The direction of the cross-island water level gradient suggests that this breach formed from ocean to bay and the large estuarine deposits associated with the breaches confirmed significant bayward sediment transport. The association between water level gradient direction (bayward or seaward) and storm deposition is consistent with findings from other barrier island systems (Sherwood et al. 2014).

The ocean-to-bay water level gradient was significant for much of the study area, and yet breaches were only observed near Mantoloking, so some other factors, such as island and estuary width, must be important. A minimum in island width (<400 m) is coincident with the larger breach, while minima in estuarine width were coincident with both breach locations (~300 and <300 m for the southern and northern breach, respectively). This coupled with our other results suggests that the formation of the breaches at Mantoloking was controlled by a combination of factors including differences in dune and storm surge elevations, ocean-to-bay water level gradient, and island-estuary morphology. This is consistent with the findings of Morton (2002) and, again, highlights the importance of analyzing storm-related coastal changes in the context of both barrier island and estuarine parameters.

Barrier-Estuary Connectivity: Contrasts Between Developed and Undeveloped Shorelines

In this study, we integrate coastal topographic change data with estuarine change data to explore spatial controls on barrier island-estuary connectivity, defined herein as the transport of sediment from barrier island to estuary. The juxtaposition of undeveloped and developed barrier island regions within the study area permitted an assessment of the influence of coastal development on coupled coastal storm response. The lack of a linear relationship between barrier island losses and estuarine gains for the study area may be related to spatial controls on over-barrier transport. For developed shorelines, water and sediment can be forced around coastal infrastructure and along roads (Morton 1976, 2002), whereas for undeveloped shorelines, the landward transport of sediment may be confined to topographic lows, such as relict overwash fans or dune blowouts (Carruthers et al. 2013; Fisher and Simpson 1979). In both cases, the beach may uniformly erode but sediment may only be transported across the barrier via one or two pathways leading to spatial inconsistencies between barrier island loss and estuarine gain. This demonstrates that storm-driven barrier-island rollover is not an alongshore-uniform process, which has implications for barrier evolution in response to sea level rise.

Measures of connectivity differed between developed and undeveloped portions of the barrier. Barrier island losses were higher for undeveloped shoreline than for developed shoreline. This response could be related to sediment availability. The undeveloped barrier is characterized by some of the highest dune heights recorded for the entire study area (Sopkin et al. 2014), while the developed portion of the island is characterized by narrow beaches and less well-developed dunes (Nordstrom et al. 2000). However, despite smaller barrier island losses, estuarine accumulation adjacent to developed regions was greater than estuarine accumulation for undeveloped regions, which suggests that undeveloped portions of the barrier island may retain more sediment. The lack of back-barrier marshes in the developed region likely contribute to this difference. Though the influence of back-barrier vegetation on sediment fluxes to estuaries is not well known, coastal vegetation has been shown to reduce storm surge propagation through frictional dissipation (Wamsley et al. 2010). Therefore, it seems possible that back-barrier marshes, common in the undeveloped region, slow storm-related flows, reduce the amount of sediment entrained in the flow and thereby reduce sediment flux to the estuary. Clearly, more research is necessary in order to address the complexity of spatial controls on the transport of sediment from barrier to estuary.

Finally, our results demonstrate that island width is a key component of barrier island-estuary connectivity. Though this is not necessarily a surprising result (Leatherman 1979), it may be the first quantitative regional demonstration of this relationship. Previous work has focused on the links between back-barrier slope and landward sediment fluxes and barrier resilience to sea level rise (Lorenzo-Trueba and Ashton 2014;

Moore et al. 2010; Wolinsky and Murray 2009). However, our results suggest that alongshore variation in island width also needs to be considered, since landward fluxes are more likely to contribute to estuarine deposition behind narrower islands.

Conclusions

The landfall of Hurricane Sandy on the coast of New Jersey during a multidisciplinary study in Barnegat Bay-Little Egg Harbor estuary allowed us to integrate hydrologic and geomorphologic observations with model simulations to assess (1) storm-related morphologic and sedimentologic changes within the estuary and (2) natural and human-induced spatial controls on barrier island-estuary connectivity. Overall, there was a little measurable morphologic change within the estuary; when observed, magnitudes of change were variable alongshore. Observed spatial associations between storm-related estuarine deposition and human modification of estuarine morphology demonstrated that barrier island and estuarine land use influenced storm-related sediment deposition. Integration of sedimentologic change information with numerical modeling results allowed a rigorous assessment of estuarine process-response relationships and showed that sediments became better sorted and coarser as a result of storm-mediated wave-current interactions. Breaches in the barrier island, which accounted for 10 % of the total estuarine deposition volume, resulted from a combination of dune-surge elevation differences, ocean-to-bay water level gradients, and island and estuarine widths. In general, barrier-estuary connectivity varied with land use and island width suggesting both play important roles in storm-related over-barrier sediment transport. This study represents one of the most comprehensive assessments of estuarine and coastal extreme storm response and highlights significant alongshore variability in estuarine geomorphology, barrier island width, and land use that influences barrier island-estuary connectivity. In order to better predict not only future coastal system storm response but also barrier island response to sea level rise, accounting for alongshore variability in estuarine geomorphology, over-barrier sediment fluxes (and their fate), and island width is essential.

Acknowledgments Funding for this project was provided by the New Jersey Department of Environmental Protection and the US Geological Survey (USGS) Coastal and Marine Geology Program. For their field support during geophysical data acquisition and sediment sampling, the authors would like to acknowledge the following: Emile Bergeron, Dann Blackwood, Bill Danforth, Dave Foster, Barry Irwin, Eric Moore, Aaron Turecek, and Chuck Worley, all currently or formerly with the USGS Woods Hole Coastal and Marine Science Center. The authors would also like to acknowledge Rodolfo Troche and Emily Klipp, formerly of the USGS St. Petersburg Coastal and Marine Science Center, for lidar data processing support. Noreen Buster assisted with figures. Any use of trade, firm, or product names is for descriptive purposes only and does not imply endorsement by the U.S. Government.

References

Andrews, B.D., Defne, Z., Miselis, J.L., Ganju, N.K. 2015. Continuous terrain model for water circulation studies, Barnegat Bay, New Jersey. *U.S. Geological Survey Data Release*. doi:10.5066/F7PK0D6B.

Andrews, B.D., Miselis, J.L., Danforth, W.W., Irwin, B.J., Worley, C.R., Bergeron, E.M., Blackwood, D.S. 2015. Marine geophysical data collected in a shallow back-barrier estuary: Barnegat Bay, New Jersey. *U.S. Geological Survey Data Series*. 937, available at: doi: 10.3133/ds937.

Blake, E.S., Kimberlain, T.B., Berg, R.J., Cangialosi, J.P., Beven II, J.L. 2013. Tropical cyclone report: Hurricane Sandy (AL182102) 22–29 October 2012. *Report of the National Hurricane Center*. 12 February 2013, 157 pp.

Brasseur, L.H., Trembanis, A.C., Brubaker, J.M., Friedrichs, C.T., Nelson, T., Wright, L.D., Reay, W., Haas, L.W. 2005. Physical response of the York River estuary to Hurricane Isabel. In: *Hurricane Isabel in perspective*, ed. Sellner, K.G., 57–63. Edgewater, MD: CRC Publication 05–160, Chesapeake Bay Research Consortium.

Carruthers, E.A., D.P. Lane, R.L. Evans, J.P. Donnelly, and A.D. Ashton. 2013. Quantifying overwash flux in barrier systems: an example from Martha's Vineyard, Massachusetts, USA. *Marine Geology* 343: 15–28.

Church, J.A., and N.J. White. 2011. Sea-level rise from the late 19th to early 21st century. *Surveys in Geophysics* 32: 585–602.

Collias, E.E., M.R. Rona, D.A. McManus, and J.S. Creager. 1963. Machine processing of geological data. *University of Washington Technical Report* 87: 119.

Davis, Jr., R.A., S.C. Knowles, and M.J. Bland. 1989. Role of hurricanes in the Holocene stratigraphy of estuaries: examples from the Gulf Coast of Florida. *Journal of Sedimentary Petrology* 59(6): 1052–1061.

Defne, Z., and N.K. Ganju. 2014. Quantifying the residence time and flushing characteristics of a shallow, back-barrier estuary: application of hydrodynamic and particle tracking models. *Estuaries and Coasts* 38(5): 1719–1734.

Dillon, W.P. 1970. Submergence effects on a Rhode Island barrier and lagoon inferences on migration of barriers. *Journal of Geology* 78: 94–106.

Dolan, R., and P. Godfrey. 1973. Effects of Hurricane Ginger on the barrier islands of North Carolina. *Geological Society of America Bulletin* 84: 1329–1334.

Donnelly, C., N. Kraus, and M. Larson. 2006. State of knowledge on measurement and modeling of coastal overwash. *Journal of Coastal Research* 22(4): 965–991.

Edmiston, H.L., S.A. Fahrny, M.S. Lamb, L.K. Levi, J.M. Wanat, J.S. Avant, K. Wren, and N.C. Selly. 2008. Tropical storm and hurricane impacts on a Gulf Coast estuary: Apalachicola Bay, Florida. *Journal of Coastal Research* S.I. 55: 38–49.

Fisher, J.J., and E.J. Simpson. 1979. Washover and tidal sedimentation rates as environmental factors in development of a transgressive barrier shoreline. In *Barrier islands from the Gulf of St. Lawrence to the Gulf of Mexico*, ed. S.P. Leatherman, 127–148. New York, NY: Academic Press, Inc.

FitzGerald, D.M., S. Penland, and D. Nummedal. 1984. Control of barrier island shape by inlet sediment bypassing: East Frisian Islands, West Germany. *Marine Geology* 60(1–4): 355–376.

Folk, R.L. 1974. *Petrology of sedimentary rocks*. Austin: Hemphill. **182pp**.

Godfrey, P.J., Godfrey, M.J. 1973. Comparison of geologic and geomorphic interactions between altered and unaltered barrier island systems in North Carolina. In: *Coastal geomorphology*, ed. Coates, D.S., 239–258. SUNY-Binghamton, Publications in Geomorphology.

Gotvald, A.J., Oberg, K.A. 2009. Acoustic Doppler current profiler applications used in rivers and estuaries by the U.S. Geological Survey: U.S. Geological Survey Fact Sheet 2008–3096.

Gregory, J.M., N.J. White, J.A. Church, M.F.P. Bierkens, J.E. Box, M.R. van den Broeke, J.G. Cogley, X. Fettweis, E. Hanna, P. Huybrechts, L.F. Konikow, P.W. Leclercq, B. Marzeion, J. Oerlemans, M.E. Tamisiea, Y. Wada, L.M. Wake, and R.S.W. van de Wal. 2013. Twentieth-century global-mean sea-level rise: is the whole greater than the sum of the parts? *Journal of Climate* 26: 4476–4499.

Hall, T.M., and A.H. Sobel. 2013. On the impact angle of Hurricane Sandy's New Jersey landfall. *Geophysical Research Letters* 40: 2312–2315. doi:10.1002/grl.50395.

Hawkes, A.D., and B.P. Horton. 2012. Sedimentary record of storm deposits from Hurricane Ike, Galveston and San Luis Islands, Texas. *Geomorphology* 171–172: 180–189. doi:10.1016/j.geomorph.2012.05.017.

Hoppe, H.L. 2007. New Jersey tide telemetry system: U.S. Geological Survey Fact Sheet 2007–3064.

Houser, C., Hamilton, S., Oravetz, J., Meyer-Arendt, K. 2007. EOF analysis of morphological change during Hurricane Ivan, *Coastal Sediments 2007*.

Houser, C., C. Hapke, and S. Hamilton. 2008. Controls on coastal dune morphology, shoreline erosion and barrier island response to extreme storms. *Geomorphology* 100: 223–240.

Isphording, W.C., D. Imsand, and G.C. Flowers. 1987. Storm-related rejuvenation of a northern Gulf of Mexico Estuary. *Gulf Coast Association of Geological Societies Transactions* 37: 357–370.

Israel, A.M., and F.G. Ethridge. 1987. A sedimentologic description of a microtidal, flood-tidal delta, San Luis Pass, Texas. *Journal of Sedimentary Petrology* 57(2): 288–300.

Kennish, M.J. 2001. Physical description of the Barnegat Bay-Little Egg Harbor estuarine system. *Journal of Coastal Research* S.I. 32: 13–27.

Knutson, T.R., J.L. McBride, J. Chan, K. Emanuel, G. Holland, C. Landsea, I. Held, J.P. Kossin, A.K. Srivastava, and M. Sugi. 2010. Tropical cyclones and climate change. *Nature Geoscience* 3: 157–163.

Leatherman, S.P. 1979. Migration of Assateague Island, Maryland, by inlet and overwash processes. *Geology* 7(2): 104–107.

Lentz, E.E., C.J. Hapke, H.F. Stockdon, and R.E. Hehre. 2013. Improving understanding of near-term barrier island evolution through multi-decadal assessment of morphologic change. *Marine Geology* 337: 125–139.

Li, M., L. Zhong, W.C. Boicourt, S. Zhang, and D.-L. Zhang. 2007. Hurricane-induced destratification and restratification in a partially-mixed estuary. *Journal of Marine Research* 65: 169–192.

Lorenzo-Trueba, J., and A.D. Ashton. 2014. Rollover, drowning, and discontinuous retreat: distinct modes of barrier response to sea-level rise arising from a simple morphodynamic model. *Journal of Geophysical Research-Earth Surface* 119: 779–801. doi:10.1002/2013JF002941.

Madsen, O.S. 1994, Spectral wave-current bottom boundary layer flows. Paper presented at 24th International Conference. Kobe, Japan: Coastal Eng. Res. Counc.

Mallin, M.A., and C.A. Corbett. 2006. How hurricane attributes determine the extent of environmental effects: multiple hurricanes and different coastal systems. *Estuaries and Coasts* 29(6A): 1046–1061.

Mallin, M.A., M.H. Posey, G.C. Shank, M.R. McIver, S.H. Ensign, and T.D. Alphin. 1999. Hurricane effects on water quality and benthos in the Cape Fear watershed: natural and anthropogenic impacts. *Ecological Applications* 9(1): 350–362.

McBride, R.A., M.R. Byrnes, and M.W. Hiland. 1995. Geomorphic response-type model for barrier coastlines: a regional perspective. *Marine Geology* 126(1–4): 143–159.

McBride, R.A., Anderson, J.B., Buynevich, I.V., et al. 2013. Morphodynamics of barrier systems: a synthesis. In: *Treatise on geomorphology*, eds. Shroder, J., Sherman, D.J. Diego, CA: Academic Press, San vol. 10, Coastal and Submarine Geomorphology, 166–244.

Moore, L.J., List, J.H., Williams, S.J., Stolper, D. 2010. Complexities in barrier island response to sea-level rise: insights from numerical model experiments, North Carolina outer banks. *Journal of Geophysical Research* 115:F03004. doi: 10.1029/2009JF001299.

Morton, R.A. 1976. Effects of Hurricane Eloise on beach and coastal structures, Florida Panhandle. *Geology* 4: 277–280.

Morton, R.A. 2002. Factors controlling storm impacts on coastal barriers and beaches—a preliminary basis for near real-time forecasting. *Journal of Coastal Research* 18: 486–501.

Moser, F.C. 1997. *Sources and sinks of nitrogen and trace metals and benthic macrofauna assemblages in Barnegat Bay*, New Jersey. Ph.D. thesis, Rutgers University, New Brunswick, New Jersey.

Nicholson, R.S., and M.K. Watt. 1997. Groundwater flow in the unconfined aquifer of the northern Barnegat Bay watershed, New Jersey. In *Proceedings of the Barnegat Bay ecosystem workshop*, ed. G.E. Flimlin and M.J. Kennish, 31–47. Toms River: Rutgers Cooperative Extension of Ocean County.

Nordstrom, K.F., R. Lampe, and L.M. Vandemark. 2000. Reestablishing naturally functioning dunes on developed coasts. *Environmental Management* 25(1): 37–51.

Peierls, B.L., R.R. Christian, and H.W. Paerl. 2003. Water quality and phytoplankton as indicators of hurricane impacts on a large estuarine ecosystem. *Estuaries* 26(5): 1329–1343.

Pierce, J.W. 1970. Tidal inlets and washover fans. *Journal of Geology* 8: 230–234.

Poppe, L.J., A.H. Eliason, and M.E. Hastings. 2004. A visual basic program to generate sediment grain-size statistics and to extrapolate particle distributions. *Computers and Geosciences* 30(7): 791–795.

Ruhl, C.A., Simpson, M.R. 2005. Computation of discharge using the index-velocity method in tidally affected areas: U.S. Geological Survey Scientific Investigations Report 2005–5004, 31 p.

Sallenger, A.H. 2000. Storm impact scale for barrier islands. *Journal of Coastal Research* 16: 890–895.

Seabergh, W.C., M.A. Cialone, and J.W. McCormick. 1998. *Effects of inlet modifications at Barnegat Inlet*. New Jersey: U.S. Army Corps of Engineers. **Technical report**.

Shaw, J., Y. You, D. Mohrig, and G. Kocurek. 2015. Tracking hurricane-generated storm surge with washover fan stratigraphy. *Geology* 43(2): 127–130. doi:10.1130/G36460.1.

Sherwood, C.R., J.W. Long, P.J. Dickhudt, P.S. Dalyander, D.M. Thompson, and N.G. Plant. 2014. Inundation of a barrier island (Chandeleurs Islands, Louisiana, USA) during a hurricane: observed water-level gradients and modeled seaward sand transport. *Journal of Geophysical Research-Earth Surface* 119: 1498–1515. doi:10.1002/2013JF003069.

Sopkin, K.L., Stockdon, H.F., Doran, K.S., Plant, N.G., Morgan, K.L.M., Guy, K.K., Smith, K.E.L. 2014. Hurricane Sandy: observations and analysis of coastal change. *U.S. Geological Survey Open-File Report* 2014–1088:54. doi: 10.3133/ofr20141088.

Stevens, P.W., D.A. Blewett, and J.P. Casey. 2006. Short-term effects of a low dissolved oxygen event on estuarine fish assemblages following the passage of Hurricane Charley. *Estuaries and Coasts* 29(6A): 997–1003.

Stockdon, H.F., A.H. Sallenger, R.A. Holman, and P.A. Howd. 2007. A simple model for the spatially-variable coastal response to hurricanes. *Marine Geology* 238: 1–20.

Stutz, M.L., and O.H. Pilkey. 2001. A review of global barrier island distribution. *Journal of Coastal Research* SI34: 15–22.

Thieler, E.R., Young, R.S. 1991. Quantitative evaluation of coastal geomorphological changes in South Carolina after Hurricane Hug. *Journal of Coastal Research, Sp. Iss. 8, Impacts of Hurricane Hugo: September 10–22 1989* 187–200.

Valentine, P., Blackwood, D., Parolski, K. 2000. *Seabed observation and sampling system*, U.S. Geological Survey Fact Sheet, FS-142-00, http://pubs.usgs.gov/fs/fs142-00/fs142-00.pdf.

Vermeer, M., and S. Rahmstorf. 2009. Global sea level linked to global temperature. *Proceedings of the National Academy of Sciences* 106(51): 21527–21532. doi:10.1073/pnas.0907765106.

Wamsley, T.V., M.A. Cialone, J.M. Smith, J.H. Atkinson, and J.D. Rosati. 2010. The potential of wetlands for reducing storm surge. *Ocean Engineering* 37(1): 59–68. doi:10.1016/j.oceaneng.2009.07.018.

Warner, J.C., B. Armstrong, R. He, and J.B. Zambon. 2010. Development of a coupled ocean–atmosphere–wave–sediment transport (COAWST) modeling system. *Ocean Modeling* 35(3): 230–244.

Williams, C.J., J.N. Boyer, and F.J. Jochem. 2008. Indirect hurricane effects on resource availability and microbial communities in a subtropical wetland-estuary transition zone. *Estuaries and Coasts* 31: 204–214.

Wilson, M., S.D. Meyers, and M.E. Luther. 2006. Changes in the circulation of Tampa Bay due to Hurricane Frances as recorded by ADCP measurements and reproduced with a numerical ocean model. *Estuaries and Coasts* 29(6A): 914–918.

Wolinsky, M.A., Murray, A.B. 2009. A unifying framework for shoreline migration: 2. Application to wave-dominated coasts. *Journal of Geophysical Research*. 114:F01009. doi:10.1029/2007JF000856.

Wright, C.W., Troche, R.J., Klipp, E.S., Kranenburg, C.J., Fredericks, X., Nagle, D.B. 2014a. EAARL-B submerged topography—Barnegat Bay, New Jersey, pre-Hurricane Sandy, 2012. *U.S. Geological Survey Data Series* 885. doi: 885.

Wright, C.W., Troche, R.J., Kranenburg, C.J., Klipp, E.S., Fredericks, X., Nagle, D.B. 2014b. EAARL-B submerged topography—Barnegat Bay, New Jersey, post-Hurricane Sandy, 2012–2013. *U.S. Geological Survey Data Series* 887. doi: 887.